ACS APPLIED POLYMER MATERIALS

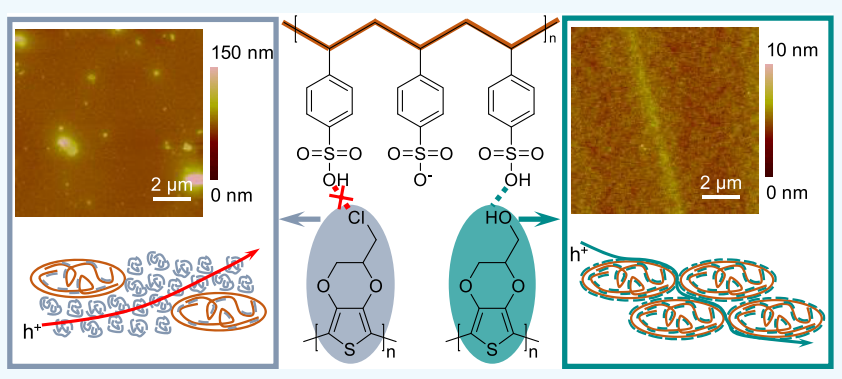
Cite This: ACS Appl. Polym. Mater. 2019, 1, 3103-3114

# Chemical Polymerization of Hydroxymethyl and Chloromethyl **Functionalized PEDOT:PSS**

Erjin Zheng, Priyesh Jain, Hao Dong, Zhiyin Niu, Shinya Chen, Shukun Zhong, and Qiuming Yu\*®

Department of Chemical Engineering, University of Washington, Seattle, Washington 98195, United States

Supporting Information



ABSTRACT: Poly(3,4-ethylenedioxythiophene) (PEDOT) conducting polymer synthesized via oxidative chemical polymerization in the presence of polyelectrolyte poly(styrenesulfonate) (PSS) can form water-dispersible conductive ink and has broad applications. However, the lack of functionality of PEDOT hinders the broader application of PEDOT:PSS. In this work, we introduced a hydroxymethyl (-MeOH) and a chloromethyl (-MeCl) functional group to the oxyethylene ring of EDOT to obtain hydroxymethylated 3,4-ethylenedioxythiophene (EDOT-MeOH) and chlorylmethylated 3,4-ethylenedioxythiophene (EDOT-MeCl) monomer, respectively. We applied oxidative chemical polymerization to synthesize PEDOT-MeCl:PSS and PEDOT-MeOH:PSS as well as PEDOT:PSS. For EDOT, we found that adding base to neutralize acidic PSS has a significant effect on the dispersibility, surface morphology, and electrical conductivity  $(9.06 \times 10^{-4} - 1.17 \times 10^{-1} \text{ S/cm})$  of PEDOT:PSS. For functionalized EDOT, the repulsive force between EDOT-MeCl monomer and PSS counterion strongly hinders the oxidation and doping process, resulting in a product with well-dispersed PSS-doped PEDOT-MeCl and nondispersible sulfatedoped PEDOT-MeCl clusters, rough thin film, and electrical conductivity of  $1.68 \times 10^{-3}$  S/cm. The hydrogen bonding between EDOT-MeOH monomer and PSS counterion as well as among EDOT-MeOH monomers makes the polymerization and doping processes easy, yielding a well-dispersed, homogeneous product, smooth thin film, and electrical conductivity of  $1.17 \times 10^{-3}$  S/cm. This study sheds light on the polymerization of PEDOT with functional groups and provides a guideline for the synthesis of functionalized PEDOT conducting polymers with polyelectrolyte counterions using oxidative chemical polymerization.

KEYWORDS: conducting polymer, PEDOT:PSS derivatives, oxidative chemical polymerization, water dispersibility, electrical conductivity, backbone chemical structures, surface morphology

# ■ INTRODUCTION

Conducting polymers have gained enormous attention since the first report in 1977. Poly(3,4-ethylenedioxythiophene) (PEDOT) is one of the most successful conducting polymers because of its flexibility, high transparency and conductivity, and great thermal and environmental stability.<sup>2</sup> PEDOT can be synthesized with different methods, such as electrochemical polymerization, transition-metal-mediated coupling polymerization, and oxidative chemical polymerization.<sup>2</sup> Electrochemical polymerization offers the advantages of the use of a small amount of monomers and short polymerization time, but the films can only be formed on conductive substrates, making it difficult to fabricate large area, uniform PEDOT thin films.<sup>3</sup> Transition-metal-mediated coupling polymerization yields neutral but typically low molecular weight PEDOT. 5,6 Oxidative chemical polymerization is considered as the most practical method because it produces PEDOT in the form of conductive ink, which can be coated onto various substrates. either conductive or nonconductive, or printed into different patterns by using an inkjet printer or other printing technologies.<sup>7,8</sup> The most commonly used PEDOT, "Baytron P", was developed by Bayer AG Company in 1988.9 The "Baytron P" was synthesized by chemically polymerizing 3,4ethylenedioxythiophene (EDOT) monomer in the presence of

Received: August 14, 2019 Accepted: October 17, 2019 Published: October 17, 2019

Scheme 1. Synthetic Route of the Chloromethyl and Hydroxymethyl Functionalized EDOT Monomers

the polyelectrolyte poly(styrenesulfonate) (PSS). The negatively charged PSS serves as the counterion to balance or to dope the positive charge of the oxidized PEDOT. In addition, the hydrophilic PSS forms a shell wrapping around the hydrophobic PEDOT core, resulting in a core—shell structure of PEDOT:PSS to be dispersed in water. Many applications of PEDOT:PSS have been developed such as solar cells, photodetectors, the light-emitting diodes, mart windows, biosensors, tuelled, biosensors, tuelled, and wearable electronics.

The conventional PEDOT:PSS, however, lacks functionality, which is particularly important in bioelectronics and biosensing. For example, the PEDOT:PSS electrode induced inflammatory response and scar formation when implanted in living tissues, thereby insulating the electrode from targeted tissues.<sup>27</sup> The functionality of PEDOT:PSS can be introduced by changing the counterion PSS or adding a functional group onto the ethylenedioxy ring in the PEDOT backbone.<sup>28</sup> PSS counterions have been replaced with other polyelectrolytes such as dextran sulfate, <sup>29</sup> heparin, <sup>30</sup> and sulfonated lignin <sup>31</sup> or small molecules such as tosylate <sup>32</sup> and chloride <sup>23</sup> to improve the PEDOT biocompatibility, conductivity, and thermoelectric properties. PEDOTs with the functional group added onto the ethylenedioxy ring are mostly polymerized from the functionalized EDOT monomer via the electrochemical polymerization method.<sup>33–35</sup> The difficulty for applying oxidative chemical polymerization to the functionalized EDOT monomers comes from the change of oxidative potential and the interaction with the oxidant and counterion because of the introduction of a functional group onto the ethylenedioxy ring. To develop functionalized PEDOT:PSS conducting polymers by using oxidative chemical polymerization method, it is crucial to understand the polymerization mechanism, especially the interaction between functionalized EDOT monomer and anionic counterion and oxidant during the reaction.

In this work, we introduced a hydroxymethyl (-MeOH) and a chloromethyl (-MeCl) functional group to the oxyethylene ring of EDOT to obtain hydroxymethylated 3,4ethylenedioxythiophene (EDOT-MeOH) and chlorylmethylated 3,4-ethylenedioxythiophene (EDOT-MeCl) monomer, respectively, and used the oxidative chemical polymerization to synthesize PEDOT:PSS, functionalized PEDOT-MeOH:PSS, and PEDOT-MeCl:PSS. In oxidative chemical polymerization, the interaction between ferric ions (Fe3+) and monomers is a critical step because Fe3+ ions first oxidize monomers to form polymers, and the couples of ferrous ions (Fe<sup>2+</sup>) and Fe<sup>3+</sup> ions catalyze the decomposition of persulfate ions  $(S_2O_8^{2-})$  into sulfate radicals  $(SO_4^{\bullet-})$  that oxidize polymers together with Fe<sup>3+</sup> ions.<sup>33,36</sup> Polyelectrolyte PSS also plays a key role in the reaction. In the initial stage of reaction, the surface charge of PSS and the interaction of PSS and monomers directly affect how Fe3+ ions attack monomers,

while in the later stage of reaction, the interaction of counterion PSS and polymers impacts the doping efficiency and dispersibility of conducting polymers. We showed that for the polymerization of EDOT the acidity of the reaction solution determines the protonation/deprotonation of PSS and the dispersibility of conducting polymers. Neutralized PSSH, by adding an equal molar of KOH, allows Fe<sup>3+</sup> ions to selectively polymerize EDOT monomers inside PSS micelles because of the electrostatic interaction of negatively charged PSS<sup>-</sup> and Fe<sup>3+</sup>, yielding PSS-doped, well-dispersed PE-DOT:PSS in water. Acidic PSSH, by adding partial or no KOH, makes Fe<sup>3+</sup> ions polymerize EDOT monomers both inside PSS micelles and in the water phase, yielding the mixtures of PSS-doped, water-dispersible PEDOT:PSS and SO<sub>4</sub><sup>2-</sup>-doped, water-nondispersible PEDOT:SO<sub>4</sub> precipitates. For the polymerization of EDOT-MeOH and EDOT-MeCl, the functional group not only changes the oxidation potential but also affects the interaction of monomers with PSS and thereby the dispersibility, conductivity, and morphology of final products. Because of the high electronegativity of -OH and -Cl, a triple amount of oxidant, compared to the polymerization of EDOT, had to be used to polymerize and oxidize PEDOT-MeOH and PEDOT-MeCl. EDOT-MeCl monomers tended to be away from PSS due to the electrostatic repulsion. As a result, PEDOT-MeCl was doped by both PSS and sulfate (SO<sub>4</sub><sup>2-</sup>), yielding a mixture of water-dispersible PEDOT-MeCl:PSS and nondispersible PEDOT-MeCl:SO4 precipitates. EDOT-MeOH monomers can form hydrogen bonding with PSS, making EDOT-MeOH monomers stay inside PSS micelles or closer to PSS. Therefore, PEDOT-MeOH polymers were mainly doped by PSS, yielding a homogeneous PEDOT-MeOH:PSS-water mixture. We further studied the surface morphology, oxidation level, and the conductivity of synthesized conducting polymers and correlated them to the proposed polymerization mechanisms.

# **■ EXPERIMENTAL SECTION**

**Materials.** 3,4-Ethylenedioxythiophene (EDOT, 97%), sodium persulfate (Na<sub>2</sub>S<sub>2</sub>O<sub>8</sub>, ≥98%), iron(III) sulfate hydrate (Fe<sub>2</sub>(SO<sub>4</sub>)<sub>3</sub>, 97%), poly(4-styrenesulfonic acid) solution (PSSH,  $M_{\rm w} \sim 75000$ , 18 wt % in H<sub>2</sub>O), hydrochloric acid (HCl, 37 wt %), 3,4-dimethoxythiophene (97%), 3-chloro-1,2-propanediol (98%), *p*-toluenesulfonic acid monohydrate (PTSA, ≥98.5%), toluene (≥99.5%), sodium acetate anhydrous (CH<sub>3</sub>COONa, >99%), and dimethyl sulfoxide (DMSO, ≥99.9%) were purchased from Sigma-Aldrich. Potassium hydroxide (KOH), dichloromethane (DCM), sodium hydroxide (NaOH), and chloroform-d (CDCl<sub>3</sub>) were purchased from Fisher Scientific. Cation exchanger LEWATIT S108H and anion exchanger LEWATIT MP62 were kindly provided by LANXESS. Commercial PEDOT:PSS Clevios P VP AI 4083 was purchased from Heraeus. All the materials were used as received without further purification.

**Synthesis of Functionalized EDOT Monomers.** The synthetic route of functionalized EDOT monomers is illustrated in Scheme 1.

The experimental details were adopted from previous studies with some modification. <sup>37,38</sup> (a) 3,4-Dimethoxythiophene (5 g), 3-chloro-1,2-propanediol (12 g), PTSA (0.676 g), and toluene (118 mL) were added into a three-neck flask. The system was purged with N2 flow for 30 min and stirred vigorously at 95 °C under N<sub>2</sub> protection for 24 h. After the removal of toluene under reduced pressure, the residue was purified by column chromatography (silica gel, hexane/DCM = 8/2 v/v) to give the product 1, 2-(chloromethyl)-2,3-dihydrothieno[3,4b][1,4]dioxine (EDOT-MeCl). <sup>1</sup>H NMR (300 MHz, CDCl<sub>3</sub>, ppm):  $\delta$  6.38 (s, 2H, Th), 4.42-4.14 (m, 3H, -O-CH<sub>2</sub>-CH-O-), and 3.65-3.78 (m, 2H,  $-CH_2-Cl$ ). The yield of EDOT-MeCl was 46%. (b) EDOT-MeCl (0.5 g),  $CH_3COONa$  (0.323 g), and DMSO (7.9 mL) were added into a flask. The solution mixture was stirred at 120 °C for 2 h. The mixture was poured into DI water (15 mL) and extracted with DCM (60 mL). (c) After the removal of DCM under reduced pressure, product 2 was added to a solution of NaOH (0.367 g) in DI water (10.5 mL). The mixture was refluxed for 1 h and then cooled to room temperature, and DI water (5.8 mL) was added. The mixture was acidified and extracted with DCM. The solvent was removed under reduced pressure, and column chromatography (silica gel, hexane/DCM = 8/2 v/v) was performed to give the product 3, 2-(hydroxymethyl)-2,3-dihydrothieno[3,4-b][1,4]dioxine (EDOT-MeOH).  $^{1}$ H NMR (300 MHz, CDCl<sub>3</sub>, ppm):  $\delta$  6.36 (s, 2H, Th), 4.08-4.27 (m, 3H, -O-CH<sub>2</sub>-CH-O-), and 3.85-3.92 (m, 2H, -CH<sub>2</sub>-OH). The step and global yield of EDOT-MeOH was 78% and 36%, respectively.

Oxidative Chemical Polymerization. PSSH (3 mL) was mixed with DI water (21 mL) for 20 min. Various molar amounts of KOH were dissolved in DI water (2 mL) and added into the mixture solution. EDOT (0.1 g) or an equal molar amount of functionalized EDOT was added into the mixture solution and stirred vigorously for 20 min to form an emulsion (Figure S1). Na<sub>2</sub>S<sub>2</sub>O<sub>8</sub> (0.25 g for EDOT or 0.75 g for functionalized EDOT) and  $Fe_2(SO_4)_3$  (0.00187 g for EDOT or 0.00561 g for functionalized EDOT) were dissolved in DI water (1 mL) and added into the emulsion sequentially. The emulsion was stirred vigorously under room temperature for 24 h until the UV-vis absorption intensity of the solution did not change. UV-vis absorption was collected by using a Varian Cary 5000 UV-vis-NIR spectrophotometer by diluting a 100  $\mu$ L sample with 3.5 mL of DI water. S108H and MP62 ion exchanger resins (4.5 and 6.5 g, respectively) were added into the solution, stirred for 2 h, and removed by vacuum filtration. The product solution was dark blue in color.

Fabrication and Characterization of Polymer Thin Films. Glass substrates were first cut into 15 mm × 15 mm pieces, then cleaned sequentially by sonication in soapy DI water, DI water, acetone, and isopropanol for 15 min each and then treated with 100 W oxygen plasma for 10 min. PEDOT:PSS or functionalized PEDOT:PSS was treated with ultrasound for 5 min, spin-coated onto a clean glass substrate at 1000, 3000, and 5000 rpm, and annealed at 150 °C for 10 min for Raman, conductivity, and atomic force microscope (AFM) measurements, respectively.

The morphology of PEDOT:PSS and functionalized PEDOT:PSS thin films was characterized by tapping mode AFM (TM-AFM) using a Digital Multimode AFM equipped with a Nanoscope IVa controller. Conductivity was measured by a Jandel cylindrical four-point probe connected with a Keithley 2450 SourceMeter. The film thickness was characterized by an Olympus OLS41 profilometer. Raman spectroscopic measurement was performed on Thermo Scientific DXR2 Raman microscope with a 532 nm green laser. The laser power applied was between 1 and 5 mW to avoid damaging polymer thin films, and a  $10 \times (N.A. = 0.25)$  or  $50 \times (N.A. = 0.50)$  objective lens was used to focus the laser on the sample. Raman spectra were fitted by using PeakFit with the assumption of 50% Gaussian and 50% Lorentzian component peaks.

#### RESULTS AND DISCUSSION

Oxidative Chemical Polymerization of PEDOT:PSS and Functionalized PEDOT:PSS. Scheme 2 shows the Scheme 2. Schematic Description of the Oxidative Step-Growth Polymerization of EDOT into PEDOT and Doping of PEDOT: (1) Oxidation of EDOT To Form a Cation Radical; (2) Dimerization of Cation Radical; (3) Deprotonation To Form Dimer: (4, 5) Further Polymerization from *n*-mer to (n + 1)-mer; (6) Fe<sup>3+</sup> Regeneration and SO<sub>4</sub><sup>-</sup> Radical Formation; (7, 8) Oxidation of PEDOT Backbone and Doping with PSS or SO<sub>4</sub><sup>2-</sup> Counterion, Respectively

$$H \xrightarrow{\downarrow} H \xrightarrow{\downarrow}$$

$$+ H \xrightarrow{S} H_{n-1} \longrightarrow H \xrightarrow{S} H_{n+1}$$
 (5)

$$Fe^{2+} + S_2O_8^{2-} \longrightarrow Fe^{3+} + SO_4^{2-} + SO_4^{--}$$
 (6)

H S S 
$$\stackrel{\text{Fe}^{3+}}{\longrightarrow}$$
 H S  $\stackrel{\text{S}}{\longrightarrow}$   $\stackrel{\text{H}}{\longrightarrow}$   $\stackrel{\text{S}}{\longrightarrow}$   $\stackrel{\text{H}}{\longrightarrow}$   $\stackrel{\text{S}}{\longrightarrow}$   $\stackrel{\text{S}}{\longrightarrow}$   $\stackrel{\text{H}}{\longrightarrow}$   $\stackrel{\text{S}}{\longrightarrow}$   $\stackrel{\text{H}}{\longrightarrow}$   $\stackrel{\text{S}}{\longrightarrow}$   $\stackrel{\text{H}}{\longrightarrow}$   $\stackrel{\text{H}}{\longrightarrow}$   $\stackrel{\text{S}}{\longrightarrow}$   $\stackrel{\text{H}}{\longrightarrow}$   $\stackrel{\text{H}}{\longrightarrow}$ 

reaction processes in the oxidative chemical polymerization by using EDOT as an example. Generally, Fe<sub>2</sub>(SO<sub>4</sub>)<sub>3</sub> and Na<sub>2</sub>S<sub>2</sub>O<sub>8</sub> are added in the EDOT oxidative chemical

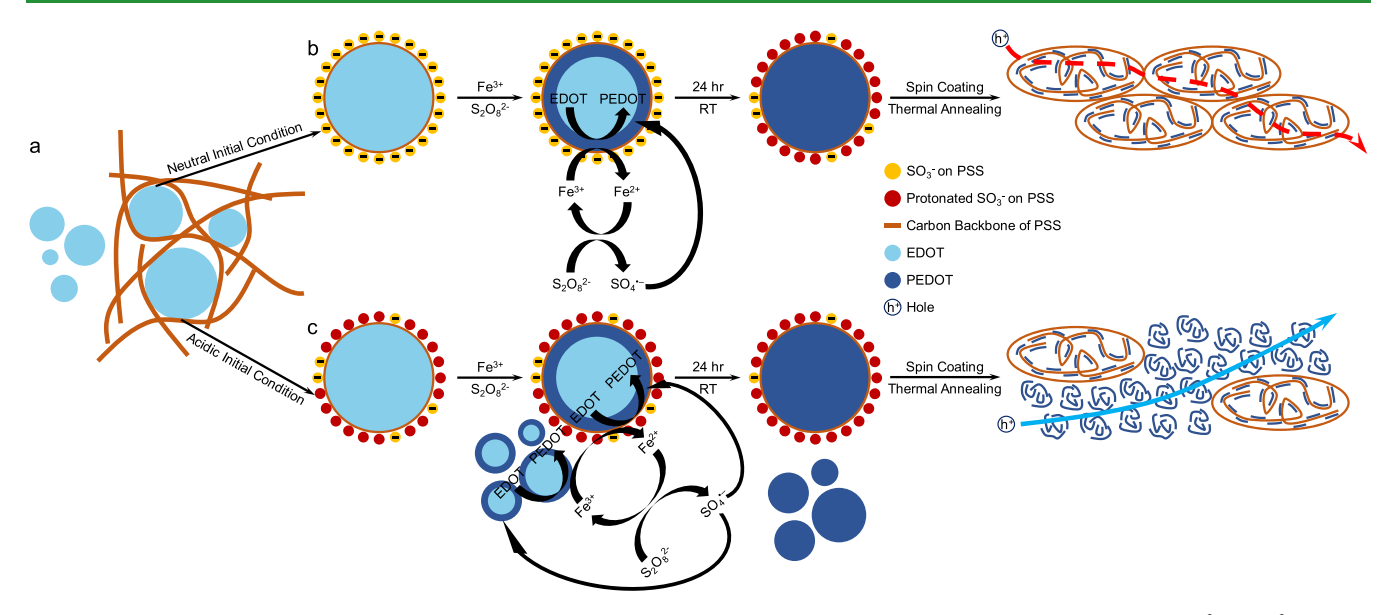


Figure 1. Schematic illustration of PEDOT:PSS polymerization mechanism under neutral and acidic initial conditions via the  ${\rm Fe}^{3+}/{\rm S}_2{\rm O}_8^{2-}$  system. (a) Initial emulsion structure of EDOT monomers and PSS chains. (b) Polymerization under a neutral initial condition achieved by adding equal molar base, resulting in the product dominated by stable, well-dispersed PSS<sup>-</sup>-doped PEDOT. Upon spin coating and thermal annealing, PEDOT:PSS grains are surrounded by PSS, which hinders the hole transport. (c) Polymerization under an acidic initial condition by adding less or no base, resulting in the product with a notable amount of nondispersible  ${\rm SO}_4^{2-}$ -doped PEDOT in addition to stable, well-dispersed PSS<sup>-</sup>-doped PEDOT. Upon spin coating and thermal annealing, PEDOT:PSS grains are surrounded by the  ${\rm SO}_4^{2-}$ -doped PEDOT polymers, which allow hole transport.

polymerization to initiate the step-growth polymerization of PEDOT and to regenerate  $Fe_2(SO_4)_3$  and oxidize PEDOT polymers, respectively.  $^{39-41}$   $Fe^{3+}$  ions oxidize an EDOT monomer into a cation radical that dimerizes and is stabilized by the removal of two protons. Dimers can also be oxidized by  $Fe^{3+}$  ions to form cation radicals and chain-growth processes as a classical stepwise polymerization. The reduced  $Fe^{2+}$  ions are oxidized by the excess amount of  $S_2O_8^{2-}$  ions, which regenerate  $Fe^{3+}$  ions and produce  $SO_4^{\bullet-}$ . The formed PEDOT polymers are oxidized by  $SO_4^{\bullet-}$  anion radicals and  $Fe^{3+}$  ions to become positively charged, which are balanced by  $PSS^-$  or  $SO_4^{2-}$  counterions.

The polyelectrolyte PSSH has a hydrophobic carbon backbone and hydrophilic sulfonic acid groups ( $-SO_3H$ ) along the backbone, resulting in a micelle-like structure in water with the carbon backbone toward the inner part of the micelles and  $-SO_3H$  groups outside. For EDOT monomers, upon addition of hydrophobic EDOT monomers, they could either diffuse into the PSSH micelles forming a dispersible emulsion or leave in water phase forming oil droplets, as illustrated in Figure 1a. Because the step-growth polymerization is initiated by Fe<sup>3+</sup> ions, deprotonation of  $-SO_3H$  groups outside the PSS micelles by adding base could affect whether the EDOT polymerization occurs preferably inside the micelles or in oil droplets in the water phase. Therefore, we proposed a base-dependent mechanism based on emulsion polymerization.

As illustrated in Figure 1b, adding equal molar base deprotonates PSSH, resulting in negatively charged micelle surfaces. The electrostatic force drives positively charged Fe<sup>3+</sup> ions to the micelle surfaces, initiating the polymerization of EDOT predominately inside the micelles. EDOT monomers in the water phase could continuously diffuse into the micelles as the polymerization processes. In the meantime, self-released protons during the polymerization protonate sulfonate

(-SO<sub>3</sub><sup>-</sup>) groups outside the micelles, reducing the driving force for Fe3+ attaching micelles surfaces and thus resulting in more polymerization in the water phase.  $SO_4^{\bullet-}$  anion radicals could diffuse into the micelles or approach PEDOT in the water phase and oxidize the polymerized PEDOT together with the Fe<sup>3+</sup> ion. The presence of -SO<sub>3</sub><sup>-</sup> groups outside the emulsion could hinder the diffusion of  $SO_4^{\bullet-}$  anion radicals into the emulsion and thus limit the oxidation of PEDOT in the emulsion. But this electrostatic effect is reduced with the -SO<sub>3</sub> groups becoming protonated during the course of polymerization. The polyelectrolyte PSS<sup>-</sup> and small SO<sub>4</sub><sup>2-</sup> serve as counterions for oxidized PEDOT in the emulsion and in the water phase, respectively. Thus, the final product under the reaction with the adding of equal molar base is dominated by dispersible PSS<sup>-</sup>-doped PEDOT mixed with a small amount of nondispersible SO<sub>4</sub><sup>2-</sup>-doped PEDOT. When the product is spin-coated on substrates and transforms into a solid state after thermal annealing, the short PEDOT chains with 6-18 segments stay attached on long PSS chains, and PSS dominates the PEDOT:PSS grain boundaries.

Without adding base, as illustrated in Figure 1c, protonated  $-SO_3H$  groups, which are outside the PSS-EDOT micelles, have no electrostatic attraction to Fe³+ ions, leading to the initiation of the polymerization of EDOT both inside the micelles and in the water phase without preference. The oxidation also occurs both in the micelles and in the water phase. As a result, the product has more nondispersible PEDOT doped by  $SO_4^{2-}$  than dispersible PSS¯-doped PEDOT. When transforming into a solid state, the  $SO_4^{2-}$ doped PEDOT polymers stay in between the PEDOT:PSS grains.

In this study, we used PSSH and adjusted the molar ratio of KOH:PSSH in the reactions, which allows us to investigate the effect of deprotonation of PSSH on the polymerization using EDOT monomer. To verify the proposed mechanism, we

Table 1. Molar Ratios of Reactants in the EDOT(-X) Polymerization and the Water Dispersibility and Color of the Products<sup>a</sup>

monomer	KOH:PSSH	PSSH:EDOT-X	Na <sub>2</sub> S <sub>2</sub> O <sub>8</sub> :EDOT-X	Fe <sub>2</sub> (SO <sub>4</sub> ) <sub>3</sub> :EDOT-X	water dispersibility	product color
EDOT	1.0	4.64	1.49	0.0067	dispersible	dark blue
	0.75	4.64	1.49	0.0067	partially dispersible	dark blue
	0.5	4.64	1.49	0.0067	partially dispersible	dark blue
	0	4.64	1.49	0.0067	partially dispersible	dark blue
	0	0 <sup>a</sup>	1.49	0.0067	nondispersible	dark blue
EDOT-MeCl	0	4.64	1.49	0.0067	partially dispersible	yellow (color of PSSH)
	1	4.64	4.47	0.0201	partially dispersible	gray-green
	0	4.64	4.47	0.0201	patrially dispersible	dark blue
EDOT-MeOH	0	4.64	1.49	0.0067	dispersible	yellow (color of PSSH)
	1	4.64	4.47	0.0201	dispersible	gray-green
	0	4.64	4.47	0.0201	dispersible	dark blue

"PSSH was not added, but an equal molar amount of HCl was added to adjust the initial pH value to be the same as that in the batch without KOH.

performed the polymerization of EDOT by adding different amounts of KOH into the solution at the beginning of reactions to control the deprotonation of PSSH. The molar ratios between KOH and PSSH are 1, 0.75, 0.5, and 0. The mass ratio between PSSH and EDOT is 6:1, which is the same as that for the commercial PEDOT:PSS AI 4083. The molar ratios of reactants are listed in Table 1. A well-dispersed darkblue solution was obtained for the PEDOT:PSS synthesized with the KOH:PSSH molar ratio of 1 because almost fully deprotonated -SO<sub>3</sub><sup>-</sup> groups make the polymerization mainly follow the process described in Figure 1b. Without addition of KOH and with the KOH:PSSH molar ratios of 0.5 and 0.75, the final dark-blue solutions have some sediments, which could be attributed to the protonated or partially protonated -SO<sub>3</sub> groups, making the process dominated by the mechanism described in Figure 1c. To verify the sediments are  $SO_4^{2-}$ doped PEDOT, a batch of reaction was conducted without adding PSSH but adding an equal molar amount of HCl. In this way, the polyelectrolyte PSS- is completely eliminated from the solution and the oxidized PEDOT can only be doped by  $SO_4^{2-}$  or  $Cl^-$ . Indeed, the product is a completely nondispersible dark-blue mixture.

The UV-vis absorption spectra of the synthesized PEDOT:PSS and commercial AI 4083 PEDOT:PSS are shown in Figure 2. The polaron and bipolaron absorption range at 700–900 and beyond 1200 nm, respectively, appear in all samples with PSS, indicating the polymerization and oxidation of PEDOT:PSS.<sup>43</sup> PEDOT synthesized without

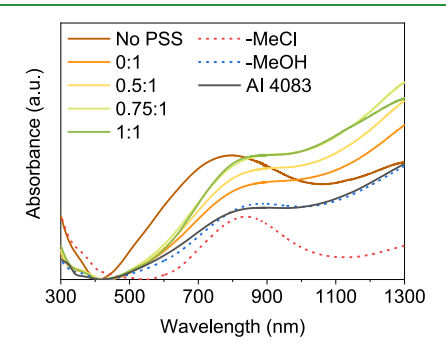


**Figure 2.** UV—vis spectra of the synthesized PEDOT:PSS with different KOH:PSSH molar ratios and without PSS, the PEDOT—MeOH:PSS and PEDOT—MeCl:PSS synthesized with no base and triple amount of oxidant, and the commercial AI 4083 PEDOT:PSS. Spectra are normalized by matching the lowest absorption point.

PSS exhibit a blue-shifted polaron absorption and reduced bipolaron absorption intensity. Because the polaron and bipolaron absorptions are due to the oxidation formed subbandgap state and the bandgap become narrower with higher oxidation level, 44,45 the blue-shifted polaron absorption and reduced bipolaron absorption intensity indicate that the PEDOT is not effectively oxidized or doped by SO<sub>4</sub><sup>2-</sup> or Cl<sup>-</sup>.

We introduced functional groups of -MeCl and -MeOH to the oxyethylene ring of EDOT and synthesized EDOT-MeCl and EDOT-MeOH monomers as shown in Scheme 1. The introduction of -MeCl and -MeOH groups to EDOT causes drastically different molecular interactions with PSS, leading to different reaction mechanisms and thus final products. As illustrated in Figure 3a, the EDOT-MeCl monomers tend to repulse either protonated or deprotonated PSS due to the high electronegativity introduced by the -MeCl functional group, making EDOT-MeCl monomers hard to diffuse into PSSH micelles. Hence, as illustrated in Figure 3b, most of the EDOT-MeCl monomers are polymerized via the step-growth polymerization initiated by Fe3+ in the water phase, and only a small amount of them are polymerized inside the PSS micelle. The strong electronegativity of -MeCl also makes it hard to be doped by negatively charged PSS<sup>-</sup> or SO<sub>4</sub><sup>2-</sup> in PSS micelles or water, respectively, due to the strong electrostatic repulsion. As a result, the final PEDOT-MeCl is lightly doped by either PSS<sup>-</sup> or SO<sub>4</sub><sup>2-</sup> counterions. When formed into a solid state, poorly SO<sub>4</sub><sup>2-</sup>-doped PEDOT-MeCl polymers stay in between PEDOT-MeCl:PSS domains. Unlike the EDOT-MeCl monomer, EDOT-MeOH can form hydrogen bonding with the oxygen or hydrogen atoms in the deprotonated or protonated sulfonate group of the PSS counterion (Figure 3c), respectively, as well as water, making EDOT-MeOH monomers easily diffuse into the PSS micelle or in the peripheral of the micelle (Figure 3d). No obvious oil droplets were formed when mixing PSSH and EDOT-MeOH in water. The step-growth polymerization predominately occurs at PSS micelles, and so does the oxidation, resulting in stable PEDOT-MeOH:PSS. When transformed into a solid state, short PEDOT-MeOH chains are attached on the PSS chain at the PEDOT-MeOH:PSS grain boundaries.

We polymerized EDOT–MeCl and EDOT–MeOH using the same molar ratios of reactants as those used in the polymerization of EDOT and without adding KOH (Table 1). However, the color of the solutions remained yellow as the color of PSSH over 24 h, indicating that no polymerization occurred. The electron-pulling effect caused by chloride or

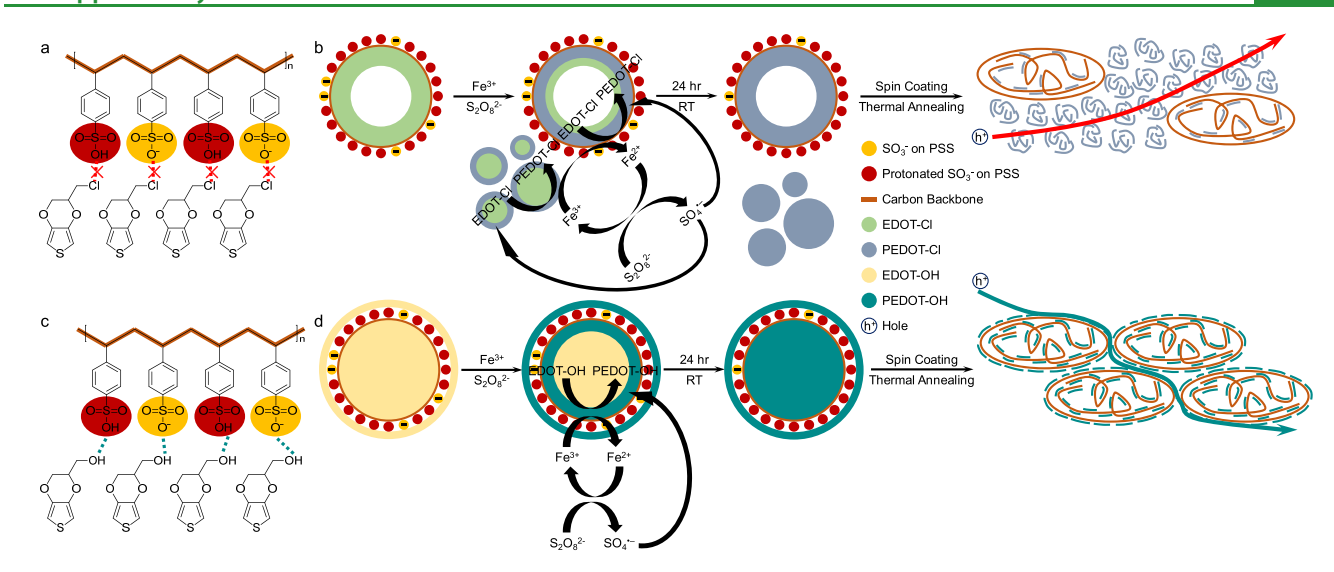
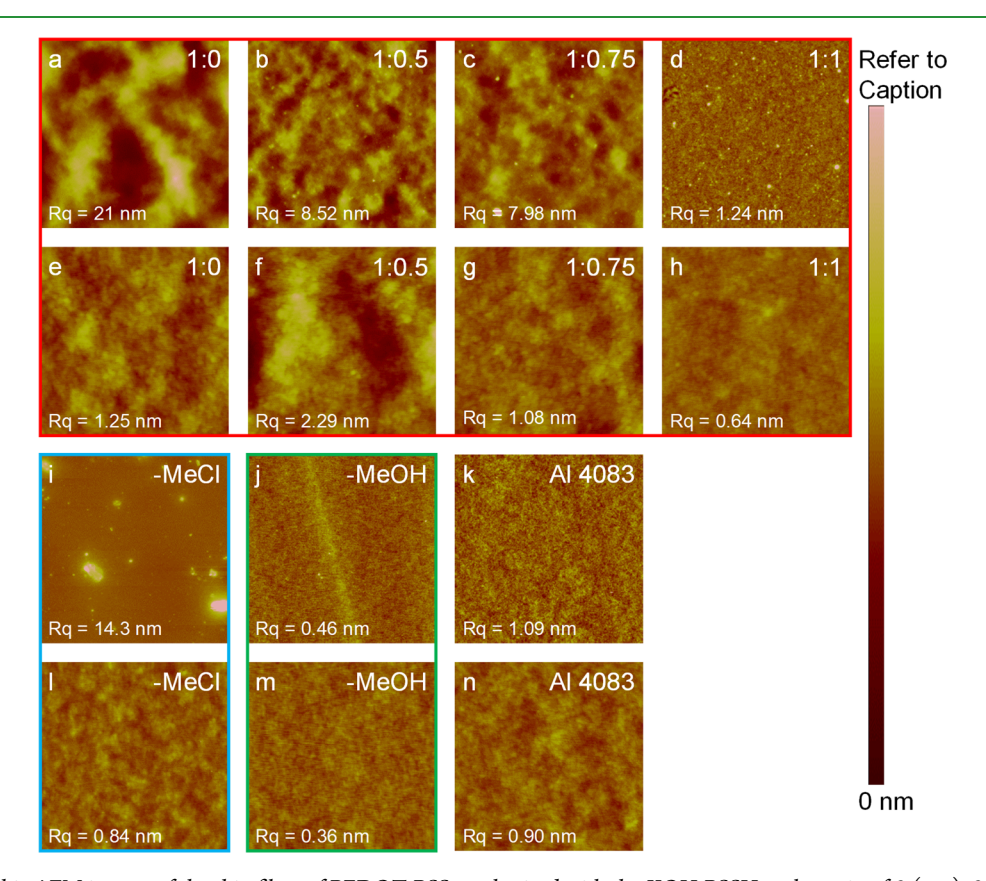


Figure 3. (a) Schematic illustration of strong repulsion between EDOT–MeCl monomer and protonated or deprotonated PSS because of the high electronegativity of the —MeCl functional group. (b) PEDOT–MeCl polymerization under an acidic initial condition, resulting in the product with a mixture of nondispersible SO<sub>4</sub><sup>2-</sup>-doped PEDOT–MeCl and stable, well-dispersed PSS<sup>-</sup>-doped PEDOT–MeCl. Upon spin coating and thermal annealing, PEDOT–MeCl:PSS grains surrounded by poorly SO<sub>4</sub><sup>2-</sup>-doped PEDOT–MeCl polymers. (c) Schematic illustration of hydrogen bonding between EDOT–MeOH monomer and protonated or deprotonated PSS. (d) PEDOT–MeOH polymerization under an acidic initial condition, resulting in stable, well-dispersed PSS<sup>-</sup>-doped PEDOT–MeOH. Upon spin coating and thermal annealing, PEDOT–MeOH:PSS domains are surrounded by PSS attached with PEDOT–MeOH, which allows hole transport through the thin layer of PEDOT–MeOH between PEDOT–MeOH:PSS domains.



**Figure 4.** Topographic AFM images of the thin films of PEDOT:PSS synthesized with the KOH:PSSH molar ratio of 0 (a, e), 0.5 (b, f), 0.75 (c, g), and 1 (d, h), PEDOT–MeCl:PSS (i, l), PEDOT–MeOH:PSS (j, m), and the commercial AI 4083 PEDOT:PSS (k, n). Image sizes are  $10 \, \mu m \times 10 \, \mu m$  for (a–d, i–k) and  $1 \, \mu m \times 1 \, \mu m$  for (e–h, l–n). The *Z* scales are as follows: for synthesized PEDOT:PSS, 150 nm (a), 100 nm (b, c), and 20 nm (d–h); for PEDOT–MeCl:PSS, 150 nm (i) and 10 nm (l); for PEDOT–MeOH:PSS, 10 nm (j, m); for commercial AI 4083 PEDOT:PSS, 20 nm (k, n).

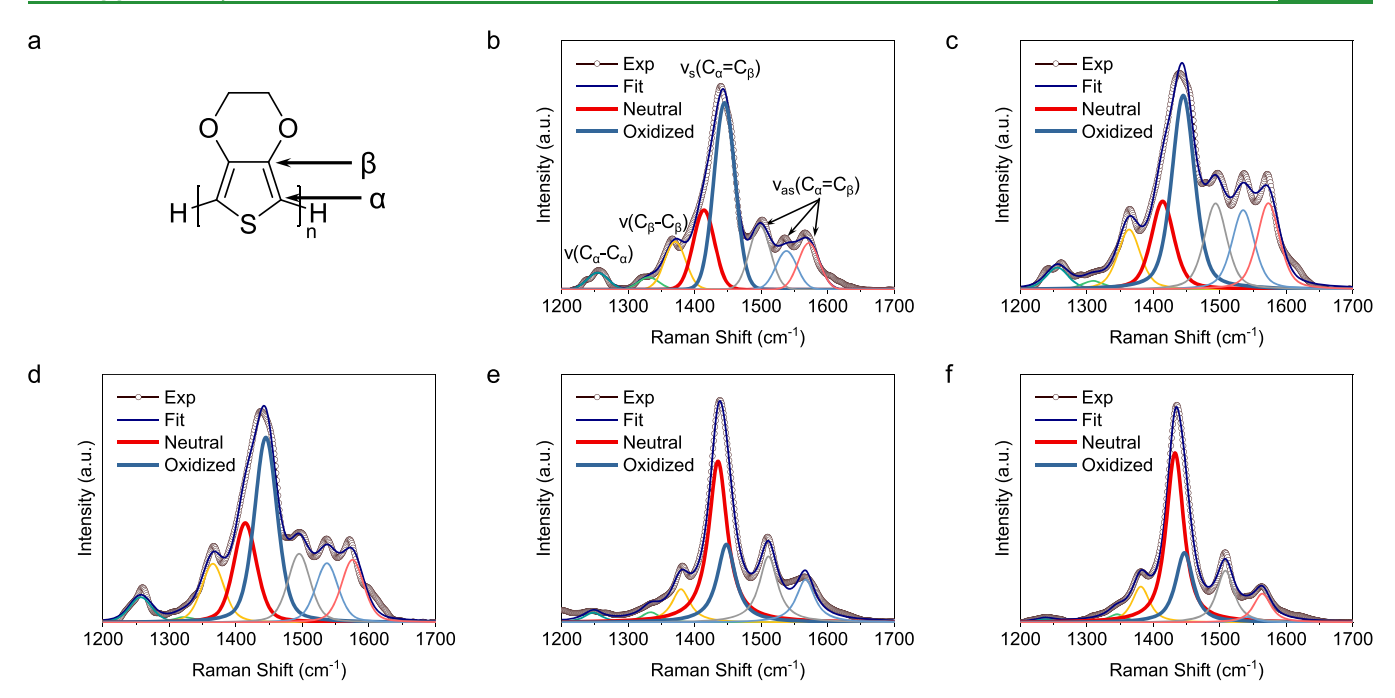


Figure 5. (a) PEDOT structure showing  $\alpha$  and  $\beta$  carbon atoms on the thiophene ring. (b-f) Raman spectra along with the spectral deconvolution of the thin films for (b) commercial AI 4083 PEDOT:PSS, PEDOT:PSS synthesized with (c) 1:1 and (d) 0:1 KOH:PSSH molar ratio, (e) PEDOT-MeCl:PSS, and (f) PEDOT-MeOH:PSS.

oxygen atom raises the oxidation potential and makes it harder to remove an electron from the monomer thiophene ring by Fe<sup>3+</sup> and SO<sub>4</sub>•- (Scheme 2). <sup>46</sup> Therefore, we tripled the molar ratios of Na<sub>2</sub>S<sub>2</sub>O<sub>8</sub> and Fe<sub>2</sub>(SO<sub>4</sub>)<sub>3</sub> to monomers and added KOH in a 1:1 KOH:PSSH molar ratio. This condition resulted in both solutions turning into a gray-green color in 24 h, indicating that short-chain PEDOT-MeCl and PEDOT-MeOH might be formed and the doping level is low. It has been reported that the acidity of the reaction solution influences the reaction kinetics, and adding base has been used to adjust the reaction kinetics. 40,47 Therefore, we conducted another batch of polymerizations by keeping the high molar ratios of  $Na_2S_2O_8$  and  $Fe_2(SO_4)_3$  to monomers but without adding KOH. Under this condition, both solutions turned dark blue in color, and the reactions were completed after 24 h. The PEDOT-MeCl:PSS solution had some precipitates while the PEDOT-MeOH:PSS solution was homogeneous. The PEDOT-MeOH:PSS solution shows both polaron and bipolaron peaks in the UV-vis absorption spectrum, similar to those in commercial AI 4083 PEDOT:PSS (Figure 2). For PEDOT-MeCl:PSS, a clear polaron absorption is shown at 700-900 nm, and a low rising bipolaron tail is present above ~1200 nm, indicating its low

Surface Morphology of PEDOT:PSS and Functionalized PEDOT:PSS. Surface morphologies of the thin films of synthesized PEDOT:PSS, PEDOT–MeCl:PSS, and PEDOT–MeOH:PSS as well as commercial AI 4083 PEDOT:PSS coated on glass substrates were characterized by using TM-AFM. To gain the surface morphology of each sample, we acquired both large area (10  $\mu$ m × 10  $\mu$ m) and small area (1  $\mu$ m × 1  $\mu$ m) topographic AFM images, which are shown in Figure 4.

The impact of adding KOH in the polymerization of PEDOT:PSS on the final products can be observed from the surface morphology of thin films. The thin film of the

PEDOT:PSS synthesized without adding KOH exhibits a very rough surface morphology presenting elongated aggregates with the height exceeding 100 nm and a root mean square roughness  $(R_a)$  of 21 nm in the large area image (Figure 4a) because of the existence of  $SO_4^{2-}$ -doped nondispersible PEDOT, as illustrated in Figure 1c. Adding KOH in the polymerization solution improves the surface morphology gradually, showing small aggregates with the height around 50 nm and reduced  $R_a$  values of 8.52 and 7.98 nm for the thin films of the PEDOT:PSS synthesized with 0.5 and 0.75 KOH:PSSH molar ratios (Figures 4b and 4c), respectively. This also demonstrates the trend that more PEDOT polymers are doped by PSS<sup>-</sup> because the process described in Figure 1b becomes dominant. Upon further increase of the molar ratio of KOH:PSSH to 1, the morphology of the thin film was significantly improved with the surface roughness ( $R_a = 1.24$ nm) (Figure 4d), which is close to the commercial AI 4083 PEDOT:PSS ( $R_q = 1.09 \text{ nm}$ ) (Figure 4k). Figure 4d shows only some small aggregates on the surface with a height around 20 nm. Fine-line features are shown in Figures 4d and 4k, which could be due to well-dispersed PEDOT:PSS. Line features are also shown in Figures 4b and 4c, indicating more PSS-doped PEDOT in the products. Figures 4e-h,n are the small area images taken from the flat area of the large area images. PEDOT:PSS synthesized without and with 0.5 and 0.75 molar ratio KOH exhibits clear domain contrast and particle-like structures (Figures 4e-g), which refer to the PEDOT doped by  $SO_4^{2-}$  as illustrated in Figure 1c. While for commercial AI 4083 and PEDOT:PSS synthesized with a KOH:PSSH ratio of 1, no particle-like structures are observed, and the films exhibit smooth uniform morphologies with fineline structure (Figures 4h,n), which is due to the dispersible PSS-doped PEDOT, as illustrated in Figure 1b.

Figure 4i shows the large area scan AFM image of the PEDOT-MeCl:PSS thin film, which has aggregates in different sizes with height above 150 nm but a relatively

smooth background. The large aggregates are attributed to the poorly  $SO_4^{2-}$ -doped PEDOT–MeCl as described in Figure 3b. The PEDOT-MeOH:PSS thin film has a smooth and uniform morphology without any aggregates and a low  $R_a$  of 0.46 nm in the large area scan AFM image (Figure 4j). The zoomed-in image of the PEDOT-MeCl:PSS sample (Figure 41) shows domain contrast and particle-like structure similar to PEDOT:PSS synthesized without KOH, which could be attributed to the aggregated PEDOT-MeCl polymers that are poorly doped by  $SO_4^{2-}$ . The small area scan image of PEDOT-MeOH:PSS, however, shows a very smooth and uniform morphology with the lowest  $R_q$  of 0.36 nm and more fine-line features (Figure 4m), indicating well-dispersed PEDOT-MeOH along PSS.

Oxidation and Doping Level of PEDOT:PSS and Functionalized PEDOT:PSS. To further investigate the effect of KOH and functional groups on the oxidation and doping level of synthesized PEDOT:PSS and functionalized PEDOT-MeCl:PSS and PEDOT-MeOH:PSS, respectively, we acquired Raman spectra of these products as shown in Figure 5. In the spectral window of 1200-1700 cm<sup>-1</sup>, peaks are mainly due to the vibrational modes related to  $C_{\alpha}$  and  $C_{\beta}$  on the thiophene ring (Figure 5a). The Raman peak assignments of the synthesized PEDOT:PSS and the commercial AI 4083 sample are listed in Table S1 and are labeled in Figure 5b. Briefly, the peaks in the ranges of 1258-1267 and 1364-1368 cm<sup>-1</sup> refer to the  $C_{\alpha}$ – $C_{\alpha'}$  inter-ring stretching and the  $C_{\beta}$ – $C_{\beta}$ stretching, respectively. The most intense peak at 1429-1443 cm<sup>-1</sup> is related to the  $C_{\alpha} = C_{\beta}$  symmetrical stretching, which can be deconvoluted into two separated bands, centered at 1414 and 1445 cm $^{-1}$  due to the  $C_{\alpha}$ = $C_{\beta}$  symmetrical stretching from the PEDOT in neutral and oxidized state, respectively. The  $C_{\alpha}$  asymmetrical stretching occupies a board range from 1496 to 1571 cm<sup>-1</sup>. The highly oxidized PEDOT usually has three  $C_{\alpha}$ = $C_{\beta}$  asymmetrical stretching peaks while the less oxidized PEDOT usually has two.<sup>51</sup> The spectra were fitted, and the ratios of oxidized to neutral (O:N) state in the PEDOT backbone of different samples were estimated from the area of the peaks corresponding to the  $C_{\alpha}$ = $C_{\beta}$  symmetry stretching modes of the oxidized and neutral states.

The thin film of PEDOT:PSS synthesized with a 1:1 KOH:PSSH molar ratio has an O:N ratio of 2.20 (Figure 5c), which is similar to the O:N ratio of 2.35 for the commercial AI 4083 PEDOT:PSS. The high O:N ratio indicates that the PEDOT is effectively oxidized and doped by PSS counterion, while the O:N ratio reduces to 1.86 (Figure 5d) for the thin film of sonicated PEDOT:PSS synthesized with a 0:1 KOH:PSSH molar ratio. We centrifuged the solution of PEDOT:PSS synthesized with a 0:1 KOH:PSSH molar ratio to separate the homogeneous solution and the sediment and acquired the Raman spectra of each part (Figures S2a,b). The thin film made from the homogeneous solution exhibits an O:N ratio of 2.62, which is higher compared with that of the thin film of AI 4083 and PEDOT:PSS synthesized with a 1:1 KOH:PSSH molar ratio. The improved O:N ratio of the 0:1 KOH:PSSH homogeneous sample is due to the higher reactivity of Fe<sup>3+</sup> and SO<sub>4</sub>•- under an acidic environment, 40,52,53 which makes the PEDOT highly oxidized. However, the sediment exhibits a much lower O:N ratio of 1.32. The low O:N ratio of the sediment might be attributed to the bivalent  $SO_4^{\ 2-}$  counterions cannot effectively dope the oxidized PEDOT, <sup>49</sup> and these small ions are easily removed in

the ion exchange process, further dedoping the PEDOT. For PEDOT synthesized without adding PSS but adding HCl, PEDOT can only be doped by small SO<sub>4</sub><sup>2-</sup> and Cl<sup>-</sup> ions. The O:N ratio further reduces to 0.71 (Figure S2c) and 0.49 (Figure S2d) before and after ion exchange, respectively. There are only two peaks shown in the  $C_{\alpha}$ = $C_{\beta}$  asymmetrical stretching range, indicating that the PEDOT is not effectively oxidized and doped. The Raman results of PEDOT without PSS agree with the observation of blue-shifted polaron absorption and low bipolaron absorption in the UV-vis spectrum (Figure 2).

With regard to functionalized PEDOT, since PEDOT-MeCl:PSS is a mixture of dispersible PSS-doped PEDOT-MeCl and nondispersible SO<sub>4</sub><sup>2-</sup>-doped PEDOT-MeCl, we collected the Raman spectra of the thin films formed from the sonicated mixture as well as from the top homogeneous solution and bottom sediment that were separated by centrifugation. The Raman peak assignments of the synthesized PEDOT-MeCl:PSS and PEDOT-MeOH:PSS samples are listed in Table S2. The  $C_{\alpha}$ - $C_{\alpha}$  inter-ring stretching peaks of functionalized PEDOT:PSS are in the range of 1240-1277 cm<sup>-1</sup>. The  $\nu(C_{\beta}-C_{\beta})$  peaks are in the range of 1379–1381 cm<sup>-1</sup>, which are blue-shifted compared to 1368 cm<sup>-1</sup> for commercial AI 4083 and synthesized PEDOT:PSS. The blueshift of  $\nu(C_{\beta}-C_{\beta})$  peaks is possibly due to the introduction of -MeCl and -MeOH functional groups, which makes the dioxy ring stiffer. The most intense peaks at 1435–1437 cm<sup>-1</sup> are also attributed to the  $C_{\alpha}$ = $C_{\beta}$  symmetrical stretching, which can be deconvoluted into neutral and oxidized PEDOT-MeCl and PEDOT-MeOH. The  $C_{\alpha}$ = $C_{\beta}$  asymmetrical stretching occupies a broad range from 1496 to 1566 cm<sup>-1</sup>. All the functionalized PEDOT-MeCl:PSS and PEDOT-MeOH:PSS samples exhibit two peaks in the  $C_{\alpha}$ =  $C_{\beta}$  asymmetrical stretching range, which indicates that the doping level is not as high as PEDOT:PSS samples even though triple amounts of Fe<sub>2</sub>(SO<sub>4</sub>)<sub>3</sub> and Na<sub>2</sub>S<sub>2</sub>O<sub>8</sub> were used.

The O:N ratios are 0.48, 0.45, and 0.54 for the films prepared with the sonicated PEDOT-MeCl:PSS mixture, the homogeneous solution, and the sediment of PEDOT-MeCl:PSS, respectively. These ratios are far below those for PEDOT:PSS. This is mainly due to the low doping level resulted from the aforementioned electron-pulling effect introduced by the -MeCl and the repulsive force between the -MeCl group and PSS<sup>-</sup> or  $SO_4^{2-}$  counterions. The  $C_\alpha$ - $C_\alpha$ inter-ring stretching peak of PEDOT-MeCl:PSS almost disappears in the top homogeneous solution while still existing centered at 1277 cm<sup>-1</sup> in the sediment. This result supports our hypothesis that EDOT-MeCl monomers are hard to form emulsions with PSS, and the step-growth polymerization of EDOT-MeCl monomers mainly takes place in the water phase, producing a relatively longer PEDOT-MeCl in the water phase. PEDOT-MeOH:PSS also shows a low O:N ratio of 0.41 because of the electron-pulling effect introduced by -MeOH, making PEDOT-MeOH hard to be oxidized. The  $C_{\alpha}$ - $C_{\alpha}$  inter-ring stretching peak for PEDOT-MeOH:PSS is slightly stronger than PEDOT-MeCl:PSS. This is mainly due to the hydrogen bonding between EDOT-MeOH monomers, making them stay close to each other and helping polymer-

Conductivity of PEDOT:PSS and Functionalized **PEDOT:PSS.** The protonation states of PSS related different reaction processes also impact the conductivity of PE-DOT:PSS thin films. The thin films of synthesized

PEDOT:PSS were made by spin coating the sonicated PEDOT:PSS solutions, including precipitates, for conductivity measurements. The conductivity of the thin film of each sample was measured through the four-point probe measurement and is plotted in Figure 6. The conductivity of

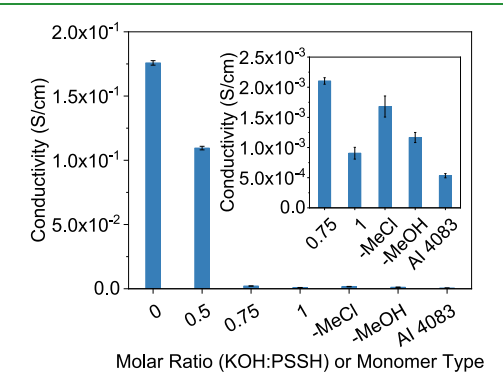


Figure 6. Conductivity of the thin films of the PEDOT:PSS synthesized with various KOH:PSSH molar ratios, PEDOT-MeCl:PSS, PEDOT-MeOH:PSS, and commercial AI 4083 PE-DOT:PSS. The inset displays the zoomed-in graph for five samples with low conductivities.

synthesized PEDOT:PSS thin films decreased with the increasing of KOH:PSSH molar ratio. The conductivity exhibited the highest value of  $1.76 \times 10^{-1}$  S/cm for the thin film synthesized without adding KOH. The conductivity decreased slightly to 1.10× 10<sup>-1</sup> S/cm by adding KOH with the KOH:PSSH molar ratio of 0.5 and further decreased significantly by 2-3 orders of magnitude to the values of 2.10  $\times$  10<sup>-3</sup> and 9.06  $\times$  10<sup>-4</sup> S/cm when the molar ratio of KOH:PSSH was increased to 0.75 and 1, respectively.

Basically, the electrical conductivity ( $\sigma$ ) is the product of carrier charge (e), carrier concentration (n) (cm $^{-3}$ ), and carrier mobility  $\mu$  (cm<sup>2</sup> V<sup>-1</sup> s<sup>-1</sup>), expressed as  $\sigma = ne\mu$ , where e is a constant and n and u can be modified via varying polymerization conditions. As  $\pi$ -conjugated polymers, the carrier concentration and carrier mobility of PEDOT, PEDOT-MeCl, and PEDOT-MeOH are highly determined by the oxidative state, the chain length, and the coplane and packing of the polymer backbone. In addition, because PEDOT, PEDOT-MeCl, and PEDOT-MeOH are doped by PSS or SO<sub>4</sub><sup>2-</sup>, the structure and morphology of the polymer complex place an important role in determining the electrical conductivity. Previous studies showed that the conductivity of PEDOT thin films is mainly determined by the charge carrier hopping distance between PEDOT backbones, or carrier mobility, which is strongly affected by the amount of counterions, especially whether the counterions are polyelectrolytes or small anions.<sup>47</sup> The doping level, or carrier concentration, has relatively less impact on the conductivity since the oxidation level of PEDOT is limited.<sup>47</sup> Some posttreatments were applied to replace PSS with  $SO_4^{\ 2-}$  or organic acid, 54,55 and several orders of magnitude enhancement of conductivity were achieved. Therefore, we attribute the high conductivity of the samples synthesized without or with 0.5 molar ratio KOH to the existence of SO<sub>4</sub><sup>2-</sup>-doped PEDOT domains, which allow charge transport easily without blocking by nonconductive PSS domains (Figure 1c). For PEDOT:PSS synthesized with KOH:PSSH ratio of 0.75 or 1, the oxidized PEDOT polymers are mainly doped by nonconductive PSS-

counterions. Large, hydrophilic polyelectrolyte PSS- counterions stabilize the hydrophobic, conductive PEDOT polymers in water by forming PEDOT-core PSS-shell structures. Charge transport between PEDOT domains is significantly hindered by nonconductive PSS shells (Figure 1b), resulting in low conductivities. Commercial AI 4083 PEDOT:PSS has high water dispersibility and homogeneity and benefits from the well-formed PEDOT-core PSS-shell structure. Therefore, the commercial AI 4083 PEDOT:PSS thin film exhibits the lowest conductivity with a value of  $5.33 \times 10^{-4}$  S/cm compared to those of all synthesized PEDOT:PSS.

We measured the conductivity of the synthesized PEDOT-MeCl:PSS and PEDOT-MeOH:PSS thin films. The PEDOT-MeCl:PSS was sonicated before spin coating, and the film contains a nondispersible portion. The conductivity of PEDOT-MeCl:PSS is  $1.68 \times 10^{-3}$  S/cm, higher than that of AI 4083 PEDOT:PSS  $(5.33 \times 10^{-4} \text{ S/cm})$  while much lower than PEDOT:PSS synthesized with 0:1 KOH:PSSH ratio  $(1.76 \times 10^{-1} \text{ S/cm})$  with similar morphology. The low conductivity of PEDOT-MeCl:PSS is mainly due to the low oxidation and doping level caused by the electron-pulling -MeCl functional group. Even though the nondispersible portion was included in the sample, this portion of PEDOT-MeCl is also poorly doped by small counterion  $SO_4^{2-}$ , which does not benefit the conductivity. The conductivity of PEDOT-MeOH:PSS is  $1.17 \times 10^{-3}$  S/cm, which is higher than the conductivity AI 4083 PEDOT:PSS  $(5.33 \times 10^{-4} \text{ S/})$ cm) and PEDOT:PSS synthesized with 1:1 KOH:PSSH (9.06  $\times$  10<sup>-4</sup> S/cm) with similar smooth morphology. The increased conductivity could be due to the hole transport pathway formed by the thin layer of PEDOT-MeOH attached to the PSS shells as illustrated in Figure 3d.

#### **CONCLUSION**

In conclusion, we studied the effect of base and functional groups on the oxidative chemical polymerization of EDOT and functionalized EDOT-MeCl and EDOT-MeOH monomers and the oxidation and doping level, morphology, and conductivity of the synthesized polymer thin films. For the polymerization of EDOT, the protonation state of PSS is critical to the dispersibility and morphological and electronic properties of PEDOT:PSS. Neutralized PSSH, by adding an equal molar of KOH, allows Fe<sup>3+</sup> ions to selectively polymerize EDOT monomers inside PSS micelles, yielding PSS doped, well-dispersed PEDOT:PSS in water. These PEDOT:PSS films are smooth, but the conductivity is low  $(9.06 \times 10^{-4} \text{ S/cm})$ , in the same range of commercial AI 4083 PEDOT:PSS, because of the nonconductive PSS shells around the PEDOTdominated domains. Acidic PSSH, by adding partial or no KOH, makes Fe3+ ions polymerize EDOT monomers both inside PSS micelles and in the water phase, yielding the mixtures of PSS-doped, dispersible PEDOT:PSS and SO<sub>4</sub><sup>2-</sup>doped, nondispersible PEDOT:SO<sub>4</sub>. The films made from these products exhibit particles and 2-3 orders of magnitude enhanced conductivity  $(1.10 \times 10^{-1} \text{ and } 1.76 \times 10^{-1} \text{ S/cm})$ because of the existence of SO<sub>4</sub><sup>2-</sup>-doped PEDOT domains, which allows hole transport easily without the blocking of nonconductive PSS. All the synthesized PEDOT:PSS have relative high oxidation and doping levels, presented by the peak area ratios in the range of 2.2-2.7 corresponding to the oxidized and neutral  $C_{\alpha}$ = $C_{\beta}$  symmetrical stretching modes in Raman spectroscopy. Introducing -MeOH and -MeCl functional groups to the EDOT monomer, the electron-pulling

property of these functional groups raises the oxidative potential of the monomers, and thus a higher amount of oxidant is required for the polymerization of EDOT-MeCl and EDOT-MeOH. The repulsive force between EDOT-MeCl monomer and PSS or SO<sub>4</sub><sup>2-</sup> counterion strongly hinders the oxidation and doping process, resulting in the mixture of PSS-doped, water-dispersible PEDOT-MeCl and SO<sub>4</sub><sup>2-</sup>doped, water-nondispersible PEDOT-MeCl. The thin films of PEDOT-MeCl have large particles and low conductivity of  $1.68 \times 10^{-3}$  S/cm compared to PEDOT:PSS synthesized without adding KOH with the similar aggregation morphology. The hydrogen bonding between EDOT-MeOH monomer and PSS counterion as well as among EDOT-MeOH monomers makes the polymerization and doping processes easy, yielding PSS-doped, water-dispersible PEDOT-MeOH. The PEDOT-MeOH:PSS thin films are very smooth, and the conductivity (1.17  $\times$  10<sup>-3</sup> S/cm) is higher than commercial AI 4083 with the similar smooth morphology because of a thin layer of PEDOT-MeOH attached along the PSS in grain boundaries. The oxidation and doping levels of PEDOT-MeCl and PEDOT-MeOH are low, revealed by the low peak area ratios in the range 0.4-0.5 corresponding to the oxidized and neutral  $C_{\alpha} = C_{\beta}$  symmetrical stretching modes. This study sheds light on the polymerization of PEDOT with functional groups and provides a guideline for the synthesis of functionalized PEDOT conducting polymers with polyelectrolyte using oxidative chemical polymerization.

#### ASSOCIATED CONTENT

#### Supporting Information

The Supporting Information is available free of charge on the ACS Publications website at DOI: 10.1021/acsapm.9b00757.

Tyndall effect experiments of EDOT-PSS-water mixture, PSS-water solution, and water; Raman spectra along with the spectral deconvolution of the thin films for the top homogeneous solution and the bottom sediment of PEDOT:PSS synthesized with a 0:1 KOH:PSSH molar ratio after centrifugation, PEDOT synthesized without adding PSSH before and after ion exchange, top homogeneous solution and bottom sediment of PEDOT-MeCl:PSS after centrifugation; Raman peak assignment of the synthesized PEDOT:PSS and commercial AI 4083 PEDOT:PSS excited by a 532 nm laser; Raman peak assignment of the synthesized PEDOT-MeCl:PSS and PEDOT-MeOH:PSS thin films excited by a 532 nm laser (PDF)

### AUTHOR INFORMATION

#### **Corresponding Author**

\*E-mail: qyu@uw.edu. Phone: 206-543-4807. Fax: 206-685-3451.

#### ORCID ®

Erjin Zheng: 0000-0002-0576-5614 Qiuming Yu: 0000-0002-2401-4664

The authors declare no competing financial interest.

# **ACKNOWLEDGMENTS**

This work was supported by the National Science Foundation (CBET-1748101 and CMMI-1661660) and the Defense Threat Reduction Agency (HDTRA 1-15-1-0021). E.Z.

acknowledges the support from the State of Washington through the University of Washington Clean Energy Institute and via funding from the Washington Research Foundation. Part of this work was conducted at the Washington Clean Energy Testbeds, an open-access research facility operated by the University of Washington Clean Energy Institute. UV-vis absorption measurements were performed in the UW Department of Chemistry's Spectroscopic and Analytical Instrumentation facility.

#### REFERENCES

- (1) Shirakawa, H.; Louis, E. J.; Macdiarmid, A. G.; Chiang, C. K.; Heeger, A. J. Synthesis of Electrically Conducting Organic Polymers -Halogen Derivatives of Polyacetylene, (CH)X. J. Chem. Soc., Chem. Commun. 1977, 16, 578-580.
- (2) Groenendaal, B. L.; Jonas, F.; Freitag, D.; Pielartzik, H.; Reynolds, J. R. Poly(3,4-ethylenedioxythiophene) and its derivatives: Past, present, and future. Adv. Mater. 2000, 12 (7), 481-494.
- (3) Sotzing, G. A.; Reynolds, J. R.; Steel, P. J. Poly(3,4ethylenedioxythiophene) (PEDOT) prepared via electrochemical polymerization of EDOT, 2,2'-bis(3,4-ethylenedioxythiophene) (BiE-DOT), and their TMS derivatives. Adv. Mater. 1997, 9 (10), 795-
- (4) Yan, J.; Sun, C. H.; Tan, F. R.; Hu, X. J.; Chen, P.; Qu, S. C.; Zhou, S. Y.; Xu, J. K. Electropolymerized poly(3,4ethylenedioxythiophene):poly(styrene sulfonate) (PEDOT:PSS) film on ITO glass and its application in photovoltaic device. Sol. Energy Mater. Sol. Cells 2010, 94 (2), 390-394.
- (5) Yamamoto, T.; Abla, M. Synthesis of non-doped poly(3,4ethylenedioxythiophene) and its spectroscopic data. Synth. Met. 1999, 100 (2), 237-239.
- (6) Yamamoto, T.; Abla, M.; Shimizu, T.; Komarudin, D.; Lee, B. L.; Kurokawa, E. Temperature dependent electrical conductivity of pdoped poly(3,4-ethylenedioxythiophene) and poly(3-alkylthiophene)s. Polym. Bull. 1999, 42 (3), 321-327.
- (7) Wu, C. H.; Don, T. M.; Chiu, W. Y. Characterization and conversion determination of stable PEDOT latex nanoparticles synthesized by emulsion polymerization. Polymer 2011, 52 (6), 1375-1384.
- (8) Harman, D. G.; Gorkin, R., III; Stevens, L.; Thompson, B.; Wagner, K.; Weng, B.; Chung, J. H. Y.; Panhuis, M. I. H.; Wallace, G. G. Poly(3,4-ethylenedioxythiophene):dextran sulfate (PEDOT:DS) -A highly processable conductive organic biopolymer. Acta Biomater. 2015, 14, 33-42.
- (9) Bayer, A. G. Polythiophenes, process for their preparation and their use, 1988.
- (10) Horii, T.; Li, Y. C.; Mori, Y.; Okuzaki, H. Correlation between the hierarchical structure and electrical conductivity of PEDOT/PSS. Polym. J. 2015, 47 (10), 695-699.
- (11) Takano, T.; Masunaga, H.; Fujiwara, A.; Okuzaki, H.; Sasaki, T. PEDOT Nanocrystal in Highly Conductive PEDOT:PSS Polymer Films. Macromolecules 2012, 45 (9), 3859-3865.
- (12) Tosado, G. A.; Lin, Y. Y.; Zheng, E. J.; Yu, Q. M. Impact of cesium on the phase and device stability of triple cation Pb-Sn double halide perovskite films and solar cells. J. Mater. Chem. A 2018, 6 (36), 17426-17436.
- (13) Kaltenbrunner, M.; Adam, G.; Glowacki, E. D.; Drack, M.; Schwodiauer, R.; Leonat, L.; Apaydin, D. H.; Groiss, H.; Scharber, M. C.; White, M. S.; Sariciftci, N. S.; Bauer, S. Flexible high power-perweight perovskite solar cells with chromium oxide-metal contacts for improved stability in air. Nat. Mater. 2015, 14 (10), 1032-1039.
- (14) Li, S. X.; Zhan, L. L.; Sun, C. K.; Zhu, H. M.; Zhou, G. Q.; Yang, W. T.; Shi, M. M.; Li, C. Z.; Hou, J. H.; Li, Y. F.; Chen, H. Z. Highly Efficient Fullerene-Free Organic Solar Cells Operate at Near Zero Highest Occupied Molecular Orbital Offsets. J. Am. Chem. Soc. **2019**, 141 (7), 3073–3082.
- (15) Gao, K.; Jo, S. B.; Shi, X. L.; Nian, L.; Zhang, M.; Kan, Y. Y.; Lin, F.; Kan, B.; Xu, B.; Rong, Q. K.; Shui, L. L.; Liu, F.; Peng, X. B.;

- Zhou, G. F.; Cao, Y.; Jen, A. K. Y. Over 12% Efficiency Nonfullerene All-Small-Molecule Organic Solar Cells with Sequentially Evolved Multilength Scale Morphologies. Adv. Mater. 2019, 31 (12), 1807842.
- (16) Gao, K.; Li, L. S.; Lai, T. Q.; Xiao, L. G.; Huang, Y.; Huang, F.; Peng, J. B.; Cao, Y.; Liu, F.; Russell, T. P.; Janssen, R. A. J.; Peng, X. B. Deep Absorbing Porphyrin Small Molecule for High-Performance Organic Solar Cells with Very Low Energy Losses. J. Am. Chem. Soc. 2015, 137 (23), 7282-7285.
- (17) Zhang, X. Y.; Zheng, E. J.; Esopi, M. R.; Cai, C.; Yu, Q. M. Flexible Narrowband Ultraviolet Photodetectors with Photomultiplication Based on Wide Band Gap Conjugated Polymer and Inorganic Nanoparticles. ACS Appl. Mater. Interfaces 2018, 10 (28), 24064-
- (18) Zheng, E. J.; Zhang, X. Y.; Esopi, M. R.; Cai, C.; Zhou, B. Y.; Lin, Y. Y.; Yu, Q. M. Narrowband Ultraviolet Photodetectors Based on Nanocomposite Thin Films with High Gain and Low Driving Voltage. ACS Appl. Mater. Interfaces 2018, 10 (48), 41552-41561.
- (19) Zhang, Q.; Tavakoli, M. M.; Gu, L. L.; Zhang, D. Q.; Tang, L.; Gao, Y.; Guo, J.; Lin, Y. J.; Leung, S. F.; Poddar, S.; Fu, Y.; Fan, Z. Y. Efficient metal halide perovskite light-emitting diodes with significantly improved light extraction on nanophotonic substrates. Nat. Commun. 2019, 10, 727.
- (20) Wang, K.; Wu, H. P.; Meng, Y. N.; Zhang, Y. J.; Wei, Z. X. Integrated energy storage and electrochromic function in one flexible device: an energy storage smart window. Energy Environ. Sci. 2012, 5 (8), 8384-8389.
- (21) Khodagholy, D.; Rivnay, J.; Sessolo, M.; Gurfinkel, M.; Leleux, P.; Jimison, L. H.; Stavrinidou, E.; Herve, T.; Sanaur, S.; Owens, R. M.; Malliaras, G. G. High transconductance organic electrochemical transistors. Nat. Commun. 2013, 4, 2133.
- (22) Rivnay, J.; Inal, S.; Salleo, A.; Owens, R. M.; Berggren, M.; Malliaras, G. G. Organic electrochemical transistors. Nat. Rev. Mater. **2018**, 3 (2), 17086.
- (23) Mitraka, E.; Jafari, M. J.; Vagin, M.; Liu, X.; Fahlman, M.; Ederth, T.; Berggren, M.; Jonsson, M. P.; Crispin, X. Oxygen-induced doping on reduced PEDOT. J. Mater. Chem. A 2017, 5 (9), 4404-4412.
- (24) Winther-Jensen, B.; Winther-Jensen, O.; Forsyth, M.; MacFarlane, D. R. High rates of oxygen reduction over a vapor phase-polymerized PEDOT electrode. Science 2008, 321 (5889), 671-674
- (25) del Agua, I.; Mantione, D.; Ismailov, U.; Sanchez-Sanchez, A.; Aramburu, N.; Malliaras, G. G.; Mecerreyes, D.; Ismailova, E. DVS-Crosslinked PEDOT:PSS Free-Standing and Textile Electrodes toward Wearable Health Monitoring. Adv. Mater. Technol. 2018, 3 (10), 1700322.
- (26) Savagatrup, S.; Chan, E.; Renteria-Garcia, S. M.; Printz, A. D.; Zaretski, A. V.; O'Connor, T. F.; Rodriquez, D.; Valle, E.; Lipomi, D. J. Plasticization of PEDOT:PSS by Common Additives for Mechanically Robust Organic Solar Cells and Wearable Sensors. Adv. Funct. Mater. 2015, 25 (3), 427-436.
- (27) Zhu, B.; Luo, S. C.; Zhao, H. C.; Lin, H. A.; Sekine, J.; Nakao, A.; Chen, C.; Yamashita, Y.; Yu, H. H. Large enhancement in neurite outgrowth on a cell membrane-mimicking conducting polymer. Nat. Commun. 2014, 5, 4523.
- (28) Mantione, D.; del Agua, I.; Sanchez-Sanchez, A.; Mecerreyes, D. Poly(3,4-ethylenedioxythiophene) (PEDOT) Derivatives: Innovative Conductive Polymers for Bioelectronics. Polymers 2017, 9 (8), 354.
- (29) Hofmann, A. I.; Katsigiannopoulos, D.; Mumtaz, M.; Petsagkourakis, I.; Pecastaings, G.; Fleury, G.; Schatz, C.; Pavlopoulou, E.; Brochon, C.; Hadziioannou, G.; Cloutet, E. How To Choose Polyelectrolytes for Aqueous Dispersions of Conducting PEDOT Complexes. Macromolecules 2017, 50 (5), 1959-1969.
- (30) Mantione, D.; del Agua, I.; Schaafsma, W.; Diez-Garcia, I.; Castro, B.; Sardon, H.; Mecerreyes, D. Poly(3,4-ethylenedioxythiophene):GlycosAminoGlycan Aqueous Dispersions: Toward Electrically Conductive Bioactive Materials for Neural Interfaces. Macromol. Biosci. 2016, 16 (8), 1227-1238.

- (31) Wu, Y.; Wang, J. Y.; Qiu, X. Q.; Yang, R. Q.; Lou, H. M.; Bao, X. C.; Li, Y. Highly Efficient Inverted Perovskite Solar Cells With Sulfonated Lignin Doped PEDOT as Hole Extract Layer. ACS Appl. Mater. Interfaces 2016, 8 (19), 12377-12383.
- (32) Bubnova, O.; Khan, Z. U.; Malti, A.; Braun, S.; Fahlman, M.; Berggren, M.; Crispin, X. Optimization of the thermoelectric figure of merit in the conducting polymer poly(3,4-ethylenedioxythiophene). Nat. Mater. 2011, 10 (6), 429-433.
- (33) Karlsson, R. H.; Herland, A.; Hamedi, M.; Wigenius, J. A.; Aslund, A.; Liu, X. J.; Fahlman, M.; Inganas, O.; Konradsson, P. Iron-Catalyzed Polymerization of Alkoxysulfonate-Functionalized 3,4-Ethylenedioxythiophene Gives Water-Soluble Poly(3,4-ethylenedioxythiophene) of High Conductivity. Chem. Mater. 2009, 21 (9), 1815-1821.
- (34) Mawad, D.; Artzy-Schnirman, A.; Tonkin, J.; Ramos, J.; Inal, S.; Mahat, M. M.; Darwish, N.; Zwi-Dantsis, L.; Malliaras, G. G.; Gooding, J. J.; Lauto, A.; Stevens, M. M. Electroconductive Hydrogel Based on Functional Poly(Ethylenedioxy Thiophene). Chem. Mater. 2016, 28 (17), 6080-6088.
- (35) Hu, D.; Zhang, L.; Zhang, K.; Duan, X.; Xu, J.; Dong, L.; Sun, H.; Zhu, X.; Zhen, S. Synthesis and Characterization of PEDOT Derivative with Carboxyl Group and Its Chemo Sensing Application as Enhanced Optical Materials. J. Appl. Polym. Sci. 2015, 132 (9),
- (36) Sohn, J. S.; Patil, U. M.; Kang, S.; Kang, S.; Jun, S. C. Impact of different nanostructures of a PEDOT decorated 3D multilayered graphene foam by chemical methods on supercapacitive performance. RSC Adv. 2015, 5 (130), 107864-107871.
- (37) Segura, J. L.; Gomez, R.; Blanco, R.; Reinold, E.; Bauerle, P. Synthesis and electronic properties of anthraquinone-, tetracyanoanthraquinodimethane-, and perylenetetracarboxylic diimide-functionalized poly(3,4-ethylenedioxythiophenes). Chem. Mater. 2006, 18 (12), 2834-2847.
- (38) Lu, B.; Lu, Y.; Wen, Y.; Duan, X.; Xu, J.; Chen, S.; Zhang, L. Synthesis, Characterization, and Vitamin C Detection of a Novel L-Alanine-Modified PEDOT with Enhanced Chirality. Int. J. Electrochem. Sci. 2013, 8 (2), 2826-2841.
- (39) Im, S. G.; Gleason, K. K. Systematic control of the electrical conductivity of poly(3,4-ethylenedioxythiophene) via oxidative chemical vapor deposition. Macromolecules 2007, 40 (18), 6552-
- (40) Ha, Y. H.; Nikolov, N.; Pollack, S. K.; Mastrangelo, J.; Martin, B. D.; Shashidhar, R. Towards a transparent, highly conductive poly(3,4-ethylenedioxythiophene). Adv. Funct. Mater. 2004, 14 (6), 615 - 622.
- (41) Mueller, M.; Fabretto, M.; Evans, D.; Hojati-Talemi, P.; Gruber, C.; Murphy, P. Vacuum vapour phase polymerization of high conductivity PEDOT: Role of PEG-PPG-PEG, the origin of water, and choice of oxidant. Polymer 2012, 53 (11), 2146-2151.
- (42) Cowie, J. M. G.; Arrighi, V. Polymers: Chemistry and Physics of Modern Materials, 3rd ed.; CRC Press: Boca Raton, FL, 2007; pp 77-
- (43) Massonnet, N.; Carella, A.; Jaudouin, O.; Rannou, P.; Laval, G.; Celle, C.; Simonato, J. P. Improvement of the Seebeck coefficient of PEDOT:PSS by chemical reduction combined with a novel method for its transfer using free-standing thin films. J. Mater. Chem. C 2014, 2 (7), 1278-1283.
- (44) Bubnova, O.; Crispin, X. Towards polymer-based organic thermoelectric generators. Energy Environ. Sci. 2012, 5 (11), 9345-
- (45) Kroon, R.; Mengistie, D. A.; Kiefer, D.; Hynynen, J.; Ryan, J. D.; Yu, L. Y.; Muller, C. Thermoelectric plastics: from design to synthesis, processing and structure-property relationships. Chem. Soc. Rev. 2016, 45 (22), 6147-6164.
- (46) Pelzer, K. M.; Cheng, L.; Curtiss, L. A. Effects of Functional Groups in Redox-Active Organic Molecules: A High-Throughput Screening Approach. J. Phys. Chem. C 2017, 121 (1), 237-245.
- (47) Zotti, G.; Zecchin, S.; Schiavon, G.; Louwet, F.; Groenendaal, L.; Crispin, X.; Osikowicz, W.; Salaneck, W.; Fahlman, M.

Electrochemical and XPS studies toward the role of monomeric and polymeric sulfonate counterions in the synthesis, composition, and properties of poly(3,4-ethylenedioxythiophene). *Macromolecules* **2003**, 36 (9), 3337–3344.

- (48) Garreau, S.; Louarn, G.; Buisson, J. P.; Froyer, G.; Lefrant, S. In situ spectroelectrochemical Raman studies of poly(3,4-ethylenedioxythiophene) (PEDT). *Macromolecules* **1999**, 32 (20), 6807–6812.
- (49) Chiu, W. W.; Travas-Sejdic, J.; Cooney, R. P.; Bowmaker, G. A. Studies of dopant effects in poly(3,4-ethylenedioxythiophene) using Raman spectroscopy. J. Raman Spectrosc. 2006, 37 (12), 1354–1361.
- (50) Lapkowski, M.; Pron, A. Electrochemical oxidation of poly(3,4-ethylenedioxythiophene) "in situ" conductivity and spectroscopic investigations. *Synth. Met.* **2000**, *110* (1), 79–83.
- (51) Park, H.; Lee, S. H.; Kim, F. S.; Choi, H. H.; Cheong, I. W.; Kim, J. H. Enhanced thermoelectric properties of PEDOT: PSS nanofilms by a chemical dedoping process. *J. Mater. Chem. A* **2014**, 2 (18), 6532–6539.
- (52) Bouroushian, M. Electrochemistry of Metal Chalcogenides; Springer: Berlin, 2010.
- (53) Deleeuw, D. M.; Kraakman, P. A.; Bongaerts, P. E. G.; Mutsaers, C. M. J.; Klaassen, D. B. M. Electroplating of Conductive Polymers for the Metallization of Insulators. *Synth. Met.* **1994**, *66* (3), 263–273.
- (54) Kim, N.; Kang, H.; Lee, J. H.; Kee, S.; Lee, S. H.; Lee, K. Highly Conductive All-Plastic Electrodes Fabricated Using a Novel Chemically Controlled Transfer-Printing Method. *Adv. Mater.* **2015**, 27 (14), 2317–2323.
- (55) Fan, X.; Xu, B. G.; Wang, N. X.; Wang, J. Z.; Liu, S. H.; Wang, H.; Yan, F. Highly Conductive Stretchable All-Plastic Electrodes Using a Novel Dipping-Embedded Transfer Method for High-Performance Wearable Sensors and Semitransparent Organic Solar Cells. *Adv. Electron. Mater.* **2017**, *3* (5), 1600471.